Annals of Glaciology 33 2001

The surface energy budget in the Antarctic summer sea-ice pack

Gerd Wendler,[1] Anthony P. Worby[2]
[1]*Geophysical Institute, University of Alaska Fairbanks, Fairbanks, AK 99775-7320, U.S.A.*
[2]*Antarctic CRC and Australian Antarctic Division, Box 252-80, Hobart, Tasmania 7001, Australia*

ABSTRACT. The surface radiation budget was continuously measured in the sea-ice zone between 140° E (Terre Adélie) and 180° (McMurdo Sound) close to mid-summer, when the sea ice is disintegrating. These measurements were carried out during a cruise of the USCGC *Polar Sea* from Hobart, Tasmania, to McMurdo station, Antarctica, in 1998/99. Some of the findings are: the solar radiation is the major atmospheric energy source for the melting of ice. The sun was above the horizon for 24 h for most of the cruise. Due to a high amount of fractional cloudiness, the global radiation was somewhat reduced when compared to areas with lesser cloud cover. Mean noon values were around 400 W m^{-2}, while at midnight a value of 30 W m^{-2} was measured. Daily mean values of the net shortwave radiation varied widely, a function of the reflectivity of the surface, which is strongly dependent not only on the ice concentration, but also on the ice type (e.g. whether it is covered with snow, flooded, melting or dry). Detailed ice observations were carried out. Hourly values of the albedo varied from 6% (open water) to 84% (10/10 sea ice with a dry snow cover). The mean net longwave radiation was only modestly negative. The high amount of fractional cloud cover increased the longwave incoming radiation from the atmosphere. A mean value of −40 W m^{-2} was measured, which displayed only a very weak diurnal course. The sum of the short- and longwave radiation, the total radiation budget, showed the expected diurnal variation, with slightly negative values at night (for 6 h), and a mean maximum at solar noon of around 220 W m^{-2}. A mean daily value of 98 W m^{-2} was calculated.

INTRODUCTION

The Antarctic region plays an important role in the global climate system. The well-popularized ice–albedo feedback mechanism has been proposed as the primary impetus behind the historically observed rapid changes in climate. The total sea-ice extent in the Antarctic varies annually by >500% (Gloersen and others, 1992). These annual changes in sea-ice extent are much more pronounced in the Southern Hemisphere than in the Arctic Ocean, where the surrounding land masses limit the sea-ice extent. The important ice–albedo feedback mechanism is still not well presented in models. Our measurements might contribute to a better presentation of these processes in future models.

RADIATION BALANCE

The net radiation at the surface consists of two separate components, the long- and shortwave radiation:

$$R_{\mathrm{N}} = \mathrm{SW_{in}} - \mathrm{SW_{out}} + \mathrm{LW_{in}} - \mathrm{LW_{out}}\,, \qquad (1)$$

where $\mathrm{SW_{in}}$ is the incoming shortwave radiation, $\mathrm{SW_{out}}$ is the outgoing shortwave radiation, $\mathrm{LW_{in}}$ is the incoming longwave radiation and $\mathrm{LW_{out}}$ is the outgoing longwave radiation.

These four fluxes were measured directly for this study. Incoming and outgoing values are defined as the hemispherically integrated fluxes normal to the surface. The albedo (α) is the ratio of the outgoing to incoming shortwave radiation.

MEASUREMENTS AND INSTRUMENTATION

Continuous measurements were carried out from 15 December 1998 to 18 January 1999, during which USCGC *Polar Sea* traveled from Hobart, Tasmania, to McMurdo, Antarctica. The ship's track can be seen in Figure 1; the position of the ship is represented daily at noon, and the first serious sea ice was encountered on 19 December 1998. The sea-ice edge as of 1 January 1999 is also presented in the figure. Most of the measurements used in this study were taken from instruments mounted on the flying bridge at some 32 m a.s.l. Shortwave incoming and outgoing radiation, longwave incoming and outgoing radiation, as well as UVA (wavelength 320–380 m) and UVB (wavelength 280–320 m) incoming radiation were simultaneously taken with six separate radiometers; UVA and UVB radiation will not be discussed in this paper. For the shortwave fluxes we used Eppley PSP pyranometers. They are temperature-compensated and have a cosine response error of 1% for solar elevations of >20°; the error increases with lower solar elevations and is within 3% for elevations of 10–20°. For the incoming and outgoing infrared radiation, Eppley PIR pyrgeometers were used. The mounting of the upward-looking domes was straightforward, and relatively few obstructions in the field of view are experienced. The two downward-looking domes were mounted on a rigid aluminum boom from the flying bridge of the ship, extending 5 m from the ship and giving them a view of the sea surface. The ship's hull was thus in part in the field of view of the instruments, and can induce errors. The hull is a dark red color.

https://doi.org/10.3189/172756401781818220 Published online by Cambridge University Press

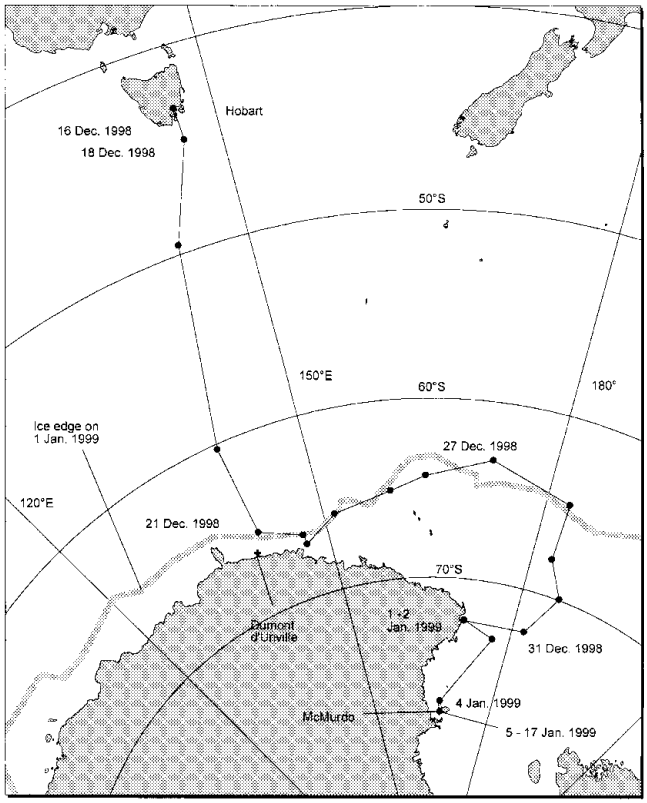

Fig. 1. The voyage of the USCGC Polar Sea *from Hobart to McMurdo, December 1998–January 1999. For selected days the position at noon is given. The ice edge as of 1 January 1999 is also shown.*

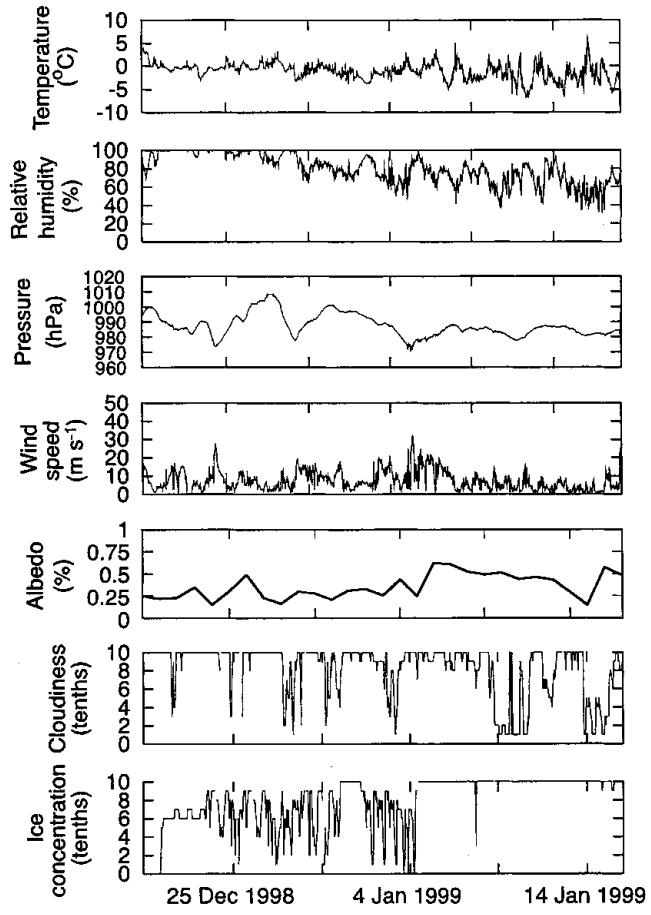

Fig. 2. Mean meteorological conditions during the cruise, December 1998–January 1999.

The effect when over open water was minor, however, when in the 10/10 sea-ice pack, too low values for the reflected flux were measured. Wendler and others (1997) made spot measurements by carrying out simultaneous observations directly over the ice and from the ship. They determined a mean error of 6% in the albedo for 10/10 ice cover, and no or small errors for open water. Further, the longwave measurements are affected. These errors could be either positive or negative, depending on the shipwall temperature in comparison to the sea-surface temperature. No corrections were carried out.

Meteorological measurements were taken. The air temperature and relative humidity was measured with a Vaisala HMP-45A probe. Atmospheric pressure was measured with a Parascientific Digiquartz pressure transducer model 216B-101. Wind speeds were taken with a Met One model 014A anemometer and a Met One wind-direction sensor model 024A. They were corrected for the movement of the ship using global positioning system measurements from a Magellen Nav5000A. Sea-surface temperature was taken with an Omega OS43L1MV infrared thermometer. Further, we measured the pitch and roll of the ship, to test how the radiative fluxes were affected by the movement of the sensors. For averaged values, which we used in this study, the effects were minor.

Each of the instruments was sampled every 2 s by a Campbell 21X datalogger. The point measurements were buffered and averaged every 5 min, then stored onto a laptop computer. With the exception of the albedo, for which mean daily values are given, hourly data are presented in Figure 2. We present the data from 19 December 1998, the day the first sea ice was observed, to 16 January 1999, omitting the first days with open water. Hourly visual observations of the ice concentration and cloud amount were carried out by the ship's crew, and are also presented in Figure 2.

RESULTS

The temperature dropped sharply in the first 2 days after leaving Hobart (Fig. 2a). However, after the sea-ice edge was reached on 20 December 1998, the air temperature remained fairly steady close to the freezing point of sea water for the first half of the journey. On 6 January 1999, we entered the fast ice of McMurdo Sound, where reduced heat transfer between the surface and the air due to the insulative effects of ice allowed the near-surface air temperature to fluctuate more strongly with the weather systems. During the voyage, three major synoptic weather events occurred around 24 and 29 December 1998 and 4 January 1999, which showed up as characteristic dips in the pressure field (971, 973 and 976 hP). Strong winds, for each case in excess of 20 m s^{-1}, accompanied these events and for the first one, high seas were observed.

In Figure 3, the mean diurnal variation of the global incoming and reflected radiation is presented for hourly averaged values, and plotted with a least-squares fitted sine curve. Given the wide range of latitudes traveled (57–78° S), these data represent averages in both time and space. The mean daily maximum in the incoming shortwave radiation is just above 400 W m^{-2}, while at night the minimum is about 40 W m^{-2}. The expected diurnal variation is observed. The mean reflected radiation reaches some 130 W m^{-2} around solar noon, indicating a mean albedo of around 30%. In Figure 4 all hourly values of the incoming solar radiation are plotted against the outgoing solar radiation for values of the incoming radiation in excess of 100 W m^{-2}. Values below this level

https://doi.org/10.3189/172756401781818220 Published online by Cambridge University Press

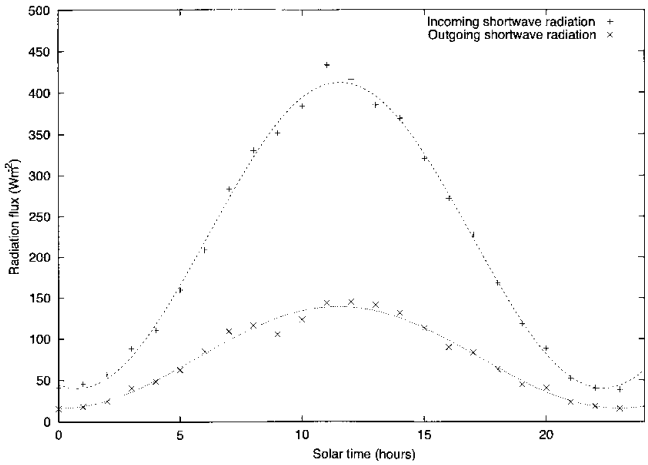

Fig. 3. Mean smoothed diurnal course of the incoming and outgoing shortwave radiation. The best sinusoidal fit is also presented.

were not used, as the albedo of water is low, and with it the outgoing shortwave flux becomes small, and absolute errors in the instrument might strongly affect the albedo values. From the whole dataset only one single hourly value was omitted as it gave an erroneous value. In Figure 4 the frequency distribution of the albedo values is also presented. Two broad maxima can be observed: one is found between 10% and 30%, typical for an open ice pack; the second is found between 40% and 60%, which represents dense pack ice. A total variation from 6% (no ice; calm water) to 84% (10/10 ice cover with dry snow) was observed. Daily mean values were 15–62%. It is rather typical that both open and dense pack are more frequently observed than the mid-range. Further, very high albedo values (>80%), which we observed

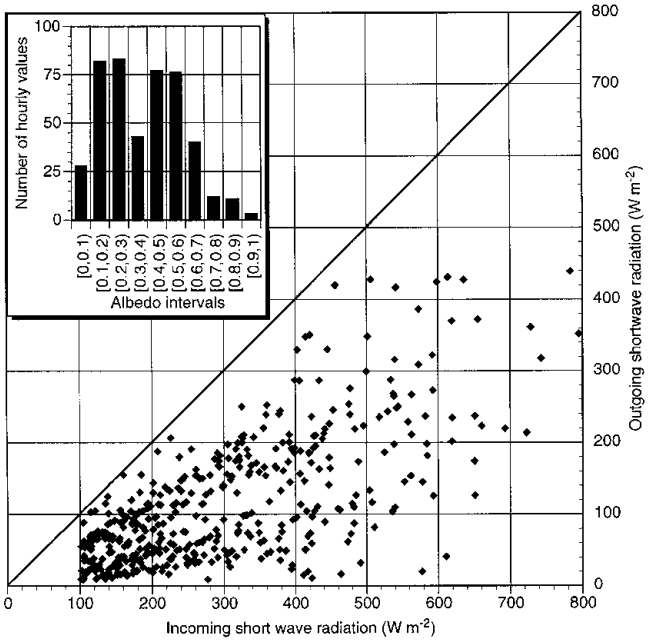

Fig. 4. Hourly values of the shortwave incoming and outgoing radiation are plotted against each other. Note that there is a large variation in the albedo, from <10% (open water) to >80% (10/10 snow-covered pack). The frequency distribution of the albedo is also presented, showing that open and dense pack are more dominant than the mid-range.

as hourly values, do not last for extended times, and mean daily values were found to be substantially lower. Allison and others (1993) reported already on this fact. If the incoming global radiation is plotted against the outgoing one (not shown), our data show a relative increase in the outgoing radiation with decreasing solar elevations. In other words, in the morning and evening hours, when the global radiation is weaker than around noon, the albedo is elevated. This is a result to be expected, as with low solar elevations the mean penetration depth of photons into a medium before being reflected is less, and hence the chances of escaping the medium are enhanced (e.g. Warren 1982).

The outgoing longwave radiation will depend, according to the Stefan–Boltzmann law, on the surface temperature and, to a lesser degree, on the surface emissivity, which is high for sea ice and water. The longwave incoming radiation depends mostly on the amount of cloud cover, cloud type and, in the absence of clouds, on the amount of water vapor, other tri-atomic gases and aerosols. When calculating the so-called atmospheric emissivity, which is the ratio of the longwave incoming to outgoing radiation, we found a value of 0.78 for clear-sky conditions. This fits quite well with values cited in the literature. For example, König-Langlo and Augstein (1994), using data from the German Antarctic expedition, gave a value of 0.765. However, the value we found for overcast conditions (0.90) is low compared to theirs (0.985). Our dataset is much smaller than theirs, so the occurrence of a few cases with high-level cloud cover may have biased our data in comparison to the long-term mean. Furthermore, our data are from close to mid-summer, hence for one season only, while the above authors had a full year of data available to deduce their constants, which are valid for the mean of the year.

The outgoing longwave radiation did not show any strong, regular, diurnal variation, indicating that the ice/ocean surface remained at a relatively constant temperature throughout the day. Nor did the longwave incoming radiation display any strong diurnal variation, a result to be expected in the absence of a pronounced diurnal variation in cloudiness. The net longwave radiation, the difference between the two values, is hence also fairly constant during the day and has a mean value of about $-40\ \mathrm{W\,m^{-2}}$. In Figure 5, this flux, the net shortwave radiation and the net radiation are presented. The shortwave flux dominates the balance, as expected during the summer season. The net longwave radiation reduces only the net radiation, the diurnal signal being little affected. On the average, we have for 6 hours daily a negative radiation budget with a minimum of $-22\ \mathrm{W\,m^{-2}}$. The maximum noon value is close to $220\ \mathrm{W\,m^{-2}}$, with a mean value for the whole trip of $98\ \mathrm{W\,m^{-2}}$.

The shortwave incoming radiation showed a dependency on the amount of cloudiness. Using our dataset and putting the best linear fit through the data points, the following regression equation could be obtained for mean daily values:

$$\mathrm{SW_{in}} = 274 - 7.3c\ [\mathrm{W\,m^{-2}}], \qquad (2)$$

where c is the fractional cloudiness in tenths. While there were many days with a high amount of cloudiness, totally clear days never occurred. The day with the least amount of cloudiness (8 January 1999) had an average of 11% cloud cover; the mean shortwave incoming radiation was $244\ \mathrm{W\,m^{-2}}$. A correlation coefficient of 0.58 was found for the equation, not a very high value. This was caused by the

https://doi.org/10.3189/172756401781818220 Published online by Cambridge University Press

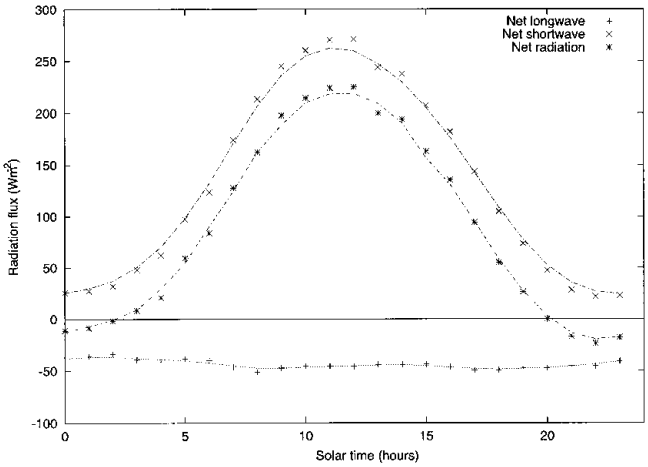

Fig. 5. Mean diurnal course of the shortwave net, longwave net and all-wave net radiation.

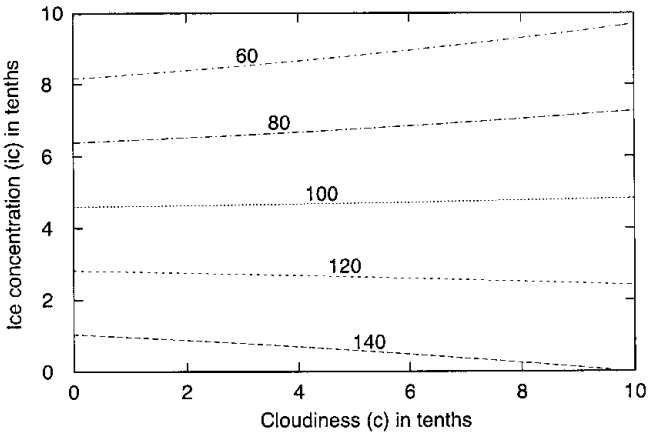

Fig. 6. The parameterized net radiation (mean daily value in $W\,m^{-2}$) as function of cloudiness and sea-ice concentration. Note the strong dependency on sea-ice concentration, and the weak one on cloud amount.

fact that not all clouds have the same transmissivity. Low clouds are normally more opaque than higher ones. However, our limited dataset did not allow the distinction between different cloud types.

The albedo is mostly dependent on the ice concentration, the best linear fit being:

$$\alpha = 14 + 4.1\mathrm{ic}\ [\%]\,, \tag{3}$$

where ic is the ice concentration in tenths. The albedo value for open water is somewhat high, as part of the time the ocean was rough and covered partly with foam. Other reasons might be high reflection due to very low solar elevations for extended times; and the reflection of the ship structure which cannot be totally discounted. For the equation a correlation coefficient of 0.65 was found. The scatter was caused by different ice types. Wendler and others (1997) showed that substantial differences can be observed for the same amount of ice concentration, depending on the ice type. However, our limited dataset did not allow the development of a regression equation which depended on both ice concentration and type.

Now, the shortwave net radiation becomes:

$$\begin{aligned} \mathrm{SW_{net}} &= \mathrm{SW_{in}} - \mathrm{SW_{out}} \\ &= (274 - 7.3c)[1 - (0.14 + 0.041\mathrm{ic})]\ [\mathrm{W\,m^{-2}}]\,. \end{aligned} \tag{4}$$

The correlation coefficient for this equation is 0.39. The longwave incoming and with it the longwave net radiation is dependent on the amount of cloudiness. Using our dataset, the best linear expression can be written as:

$$\mathrm{LW_{net}} = -84 + 5.1c\ [\mathrm{W\,m^{-2}}]\,. \tag{5}$$

The longwave net radiation has a mean value of $-84\ \mathrm{W\,m^{-2}}$ for clear-sky conditions and $-33\ \mathrm{W\,m^{-2}}$ for overcast skies. The correlation coefficient for this equation is 0.75.

The net radiation is of course the sum of the short- and longwave net radiation and can be written as:

$$\begin{aligned} R_\mathrm{N} &= \mathrm{SW_{net}} + \mathrm{LW_{net}} \\ &= (274 - 7.3c)[1 - (0.14 + 0.041\mathrm{ic})] \\ &\quad + (-84 + 5.1c)\ [\mathrm{W\,m^{-2}}]\,. \end{aligned} \tag{6}$$

For this equation, the correlation coefficient is very low (0.28), because with increasing cloudiness the net shortwave radiation decreases, while the net longwave radiation becomes less negative. In Figure 6 we show these parameterized radiation data as a function of cloudiness and sea-ice concentration. The mean net radiation shows a strong dependency on the sea-ice concentration. However, the dependency on cloudiness is weak, and only for low ice concentrations can an increase in the net radiation with decreasing cloud amount be observed. For high ice concentration (high surface albedo) the net radiation increases with increasing cloud amount, as the decrease in net shortwave radiation is overcompensated by the increased longwave incoming radiation.

DISCUSSION AND CONCLUSIONS

There are a number of studies on the radiation budget in sea ice. Most of these are carried out in the Arctic (e.g. Makshtas, 1991), and recently more work has been carried out in connection with the experiment Surface Heat Budget of the Arctic Ocean (SHEBA). In Antarctica, Weller (1968) was one of the first to carry out such measurements. The most complete radiation data were obtained by Russian North Pole drifting stations which operated from 1950 to 1991 (Marshunova and Mishin, 1994).

We found a value for the net radiation, for the average of the trip, of $98\ \mathrm{W\,m^{-2}}$. Assuming this amount is solely used for melting of sea ice, about 25 mm of sea ice could be melted daily. As the mean thickness of the sea ice surrounding Antarctica is around 40 cm, it will take on average 16 days to melt it. This can explain, of course, the sudden decay of sea ice in summer and its large variation in extent over the year. All energy does not necessarily go into melting sea ice, as the eddy fluxes can be either negative or positive (Worby and Allison, 1991). Wendler and others (1997) carried out measurements in a previous year during the same season in a similar part of the Southern Seas. They found a mean value of the net radiation of $115\ \mathrm{W\,m^{-2}}$, a value slightly higher than the one found in this study. It is believed that this is due to the lower amount of fractional cloudiness which was observed during the earlier cruise.

Comparing these measurements with measurements made in the pack ice somewhat earlier in the year (Andreas and Makshtas, 1985; Hauser and others, 1999), we found with our results a more positive net radiation budget, the combined effect of increasing solar radiation towards midsummer and a reduced surface albedo due to surface melt.

https://doi.org/10.3189/172756401781818220 Published online by Cambridge University Press

This strong seasonal variation in the radiative fluxes has, for example, been shown by Allison and others (1982) working close to Mawson, Antarctica. Once melting has occurred, the surface albedo is lowered, and future melting is accelerated. This positive feedback is even more enhanced after the snow cover has disappeared, and sea ice with a lower albedo becomes present.

Comparing our data to those from the Russian drift stations, good agreement was found only for the McMurdo Sound data. On 6 and 7 January 1999 the ship was not ice-breaking, and the sensors were steadily over 10/10 snow-covered ice. The mean incoming global radiation for these 2 days was 239 W m^{-2} and the mean albedo was 62%. The long-term mean of the Russian data for 75° N and averaged over all longitudes with measurements for July (the respective month) was 225 W m^{-2} and the mean albedo was 61%. Hence, when the ice conditions are similar, good agreement can be found between the two hemispheres.

ACKNOWLEDGEMENTS

The research was supported by U.S. National Science Foundation grant OPP 97-25843. We thank the captain and crew of the *Polar Sea* as well as the helicopter detachment which supported us wonderfully. Further, we acknowledge the help of B. Moore, J. Sheedy and H. Stone.

REFERENCES

Allison, I., C. M. Tivendale, G. J. Akerman, J. M. Tann and R. H. Wills. 1982. Seasonal variations in the surface energy exchanges over Antarctic sea ice and coastal waters. *Ann. Glaciol.*, **3**, 12–16.

Allison, I., R. E. Brandt and S. G. Warren. 1993. East Antarctic sea ice: albedo, thickness distribution, and snow cover. *J. Geophys. Res.*, **98**(C7), 12,417–12,429.

Andreas, E. L. and A. P. Makshtas. 1985. Energy exchange over Antarctic sea ice in the spring. *J. Geophys. Res.*, **90**(C4), 7199–7212.

Gloersen, P., W. J. Campbell, D. J. Cavalieri, J. C. Comiso, C. L. Parkinson and H. J. Zwally. 1992. *Arctic and Antarctic sea ice, 1978–1987: satellite passive-microwave observations and analysis*. Washington, DC, National Aeronautics and Space Administration. (NASA SP-511.)

Hauser, H., G. Wendler, U. Adolphs and M. O. Jeffries. 1999. Energy exchange in early spring over sea ice in the Pacific sector of the Southern Ocean. *J. Geophys. Res.*, **104**(D4), 3925–3935.

König-Langlo, G. and E. Augstein. 1994. Parameterisation of the downward long-wave radiation at the Earth's surface in polar regions. *Meteorol. Z.*, **3**(6), 343–347.

Makshtas, A. P. 1991. *The heat budget of the Arctic ice in the winter. English edition.* Cambridge, International Glaciological Society.

Warren, S. G. 1982. Optical properties of snow. *Rev. Geophys. Space Phys.*, **20**(1), 67–89.

Weller, G. E. 1968. The heat budget and heat transfer processes in Antarctic plateau ice and sea ice. *ANARE Sci. Rep., Ser. A(4) Glaciology* 102.

Wendler, G., U. Adolphs, A. Hauser and B. Moore. 1997. On the surface energy budget of sea ice. *J. Glaciol.*, **43**(143), 122–130.

Worby, A. P. and I. Allison. 1991. Ocean–atmosphere energy exchange over thin variable concentration Antarctic pack ice. *Ann. Glaciol.*, **15**, 184–190.

https://doi.org/10.3189/172756401781818220 Published online by Cambridge University Press